

He, C, N, and O Abundances in an Ensemble of Galactic Planetary Nebulae

Yu. V. Milanova* and A. F. Kholtygin

*Astronomical Institute, St. Petersburg State University,
Universitetskii pr. 28, St. Petersburg, 198504 Russia*

Received June 25, 2008

Abstract—The He, C, N, and O abundances in more than 120 planetary nebulae (PNe) of our Galaxy and the Magellanic Clouds have been redetermined by analyzing new PNe observations. The characteristics of PNe obtained by modeling their spectra have been used to compile a new catalog of parameters for Galactic and extragalactic PNe, which is accessible at <http://www.astro.spbu.ru/staff/afk/GalChemEvol.html>. The errors in the parameters of PNe and their elemental abundances related to inaccuracies in the observational data have been analyzed. The He abundance is determined with an accuracy of 0.06 dex, while the errors in the C, N, and O abundances are 0.1–0.2 dex. Taking into account the inaccuracies in the corrections for the ionization stages of the elements whose lines are absent in the PNe spectra increases the errors in the He abundance to 0.1 dex and in the C, N, and O abundances to 0.2–0.3 dex. The elemental abundances in PNe of various Galactic subsystems and the Magellanic Clouds have been analyzed. This analysis suggests that the Galactic bulge objects are similar to type II PNe in Peimbert's classification, whose progenitor stars belong to the thin-disk population with ages of at least 4–6 Gyr. A similarity between the elemental abundances in PNe of the Magellanic Clouds and the Galactic halo has been established.

PACS numbers : 98.35.Bd; 98.56.-p; 98.38.Ly; 98.38.Am

DOI: 10.1134/S1063773709080027

Key words: *Galaxy: evolution, subsystems; Magellanic Clouds: evolutionary status; planetary nebulae: elemental abundances*

INTRODUCTION

One of the most important objectives of investigating planetary nebulae (PNe) is their diagnostics, i.e., determining the electron temperature and density and the abundances of chemical elements and their ions in them. Determinations of elemental abundances in PNe can be used to test theories for the evolution of intermediate-mass ($1-8M_{\odot}$) stars (see, e.g., Marigo 2001; Henry 2004; Herwig 2005) and to study the chemical evolution of our Galaxy (Stanghellini et al. 2006; Matteucci 2008).

Despite the large number of papers aimed at finding PNe parameters, the accuracy of their determination and particularly the accuracy of finding elemental abundances is not yet high enough. The difference in the abundances derived by different authors can reach an order of magnitude. One of the reasons for these discrepancies is that the elemental abundances in PNe (with the exception of hydrogen and helium) are found from the intensities of collisionally excited lines, which are sensitive to the fluctuations in electron

temperature (see Peimbert and Costero 1969; Rubin 1969) and electron density (Rubin 1989) present in nebulae.

Another important factor that affects the elemental abundances derived from line intensities is a significantly different accuracy of determining the intensities of weak (compared to $H\beta$) and strong lines in the PNe spectra. The relative measurement error of the intensity increases with decreasing line intensity (see, e.g., Rola and Stasinska 1994). Rola and Pelat (1994) showed that the intensities of lines with a low signal-to-noise ratio ($S/N \leq 6$) could be overestimated by a factor of 2–6 or more.

Kholtygin (1998a) developed a technique that allowed the effects of both gas temperature and density fluctuations in PNe and different accuracy of measuring the line intensities in the PNe spectra to be taken into account. This technique proved to be efficient in analyzing the emission of a low-density astrophysical plasma, in particular, the regions of hot gas in the expanding atmospheres of hot stars (Kholtygin et al. 2003). Kholtygin (1998b, 2000) suggested a *stochastic model* of nebulae. Much more accurate

*E-mail: yulia.milanova@gmail.com

elemental abundances in nebulae than previously can be obtained by using this model.

However, a large number of new highly accurate measurements of line intensities in the PNe spectra have been performed since the publication of the cited papers. Using new observational data allows one both to improve PNe parameters for the objects considered by Kholtygin (1998a, 1998b, 2000) and to obtain these parameters for the objects for which no sufficiently reliable spectroscopic data had been available by the time the corresponding calculations were performed.

Our paper is devoted to solving this problem. In contrast to the publications by Kholtygin (1998a, 1998b, 2000), here we use more accurate atomic data, calculate the theoretical intensities of He ion lines, and determine the helium abundance in nebulae.

We provide basic formulas to calculate the line intensities in a medium with gas temperature and density fluctuations. We describe the nebular models used and the statistical procedure for determining the nebular parameters from comparison of the observed and calculated line intensities. We analyze the errors in the PNe parameters and provide the derived parameters and He, C, N, and O abundances for a large sample of Galactic nebulae. Next, we discuss the properties of an ensemble of PNe in our Galaxy and the Magellanic Clouds. In conclusion, we present some of our conclusions.

LINE INTENSITIES IN THE NEBULAR SPECTRA

To calculate the intensities of the collisionally excited intercombination, forbidden, and permitted lines of C, N, and O ions as well as the recombination lines of H and He, C, N, and O ions, we will use the method of analyzing the emission of a low-density plasma with electron temperature and density fluctuations suggested by Kholtygin (2000) and Kholtygin et al. (2003). For greater generality, we will reformulate the basic relations of the method using the concept of a *differential partial plasma emission measure* with the goal of its possible application in investigating the spectra of low-density astrophysical plasma objects of any nature.

Since the nebulae are almost always transparent in the above lines, the total energy emitted by a nebula in a particular recombination or collisionally excited $k \rightarrow i$ line of ion X^{n+} is defined by the relation

$$E_{ki} = E_{ki}(X^{n+}) = \int \int \int_V 4\pi\varepsilon_{ki} dV \quad (1)$$

$$= h\nu_{ik} \int_{T_e^1}^{T_e^2} \int_{n_e^1}^{n_e^2} r_{ki}^{\text{eff}} \mu_F(T_e, n_e) dn_e dT_e.$$

Here, ε_{ki} is the emission coefficient in the $k \rightarrow i$ line. The integration is performed over the total volume V of the plasma emitting in this line. The quantity $\mu_F(T_e, n_e)$ is the differential partial emission measure defined by the relation $\mu_F(T_e, n_e) dn_e dT_e = n_e n_F dV_{(T_e, n_e)}$, where $dV_{(T_e, n_e)}$ is the plasma volume element in which the electron temperature lies in the interval $(T_e, T_e + dT_e)$ and the electron density lies in the interval $(n_e, n_e + dn_e)$. The quantity $n_F = n(X_F)$ is the density of ion X_F whose excitation (or recombination) leads to the emission in the $k \rightarrow i$ line. $X_F \equiv X^{n+}$ for collisionally excited lines, while $X_F \equiv X^{(n+1)+}$ for recombination lines.

The effective line formation coefficient r_{ki}^{eff} is defined by the relation (Bychkov and Kholtygin 2007)

$$4\pi\varepsilon_{ki} = n_k A_{ki} h\nu_{ik} = n_e n_F r_{ki}^{\text{eff}} h\nu_{ik}. \quad (2)$$

Here, n_k is the population of level k and A_{ki} is the probability of the $k \rightarrow i$ transition.

T_e^1 and T_e^2 are, respectively, the minimum and maximum electron temperatures in the volume occupied by ion X^{n+} ; n_e^1 and n_e^2 are the minimum and maximum electron densities, respectively. The total energies emitted by a nebula in the lines can be used to find the ratios of the fluxes in the corresponding lines of the nebular spectra (corrected for the interstellar extinction).

Using the concept of a differential partial emission measure of ion X_F , we will define the total partial emission measure

$$EM_F = \int_{T_e^1}^{T_e^2} \int_{n_e^1}^{n_e^2} \mu_F(T_e, n_e) dn_e dT_e.$$

The parameters T_e and n_e averaged over the nebular volume emitting in the lines under consideration are

$$\langle T_e \rangle_F = \bar{T}_e = EM_F^{-1} \int_{T_e^1}^{T_e^2} \int_{n_e^1}^{n_e^2} T_e \mu_F(T_e, n_e) dn_e dT_e \quad (3)$$

and

$$\langle n_e \rangle_F = \bar{n}_e = EM_F^{-1} \int_{T_e^1}^{T_e^2} \int_{n_e^1}^{n_e^2} n_e \mu_F(T_e, n_e) dn_e dT_e. \quad (4)$$

Here, the averaging is performed over the distribution of the differential partial emission measure $\mu_F(T_e, n_e)$,

i.e., in general, the parameters $\overline{T_e}$ and $\overline{n_e}$ depend on the distribution of ion X_F in the nebular volume.

The parameters that characterize the rms fluctuations in T_e and n_e are defined by the formulas

$$t^2 = EM_F^{-1} \int_{T_e^1}^{T_e^2} \int_{n_e^1}^{n_e^2} (T_e - \overline{T_e})^2 \mu_F(T_e, n_e) dT_e dn_e, \quad (5)$$

$$tn = EM_F^{-1} \int_{T_e^1}^{T_e^2} \int_{n_e^1}^{n_e^2} (T_e - \overline{T_e}) \times (n_e - \overline{n_e}) \mu_F(T_e, n_e) dT_e dn_e, \quad (6)$$

$$n^2 = EM_F^{-1} \int_{T_e^1}^{T_e^2} \int_{n_e^1}^{n_e^2} (n_e - \overline{n_e})^2 \times \mu_F(T_e, n_e) dT_e dn_e. \quad (7)$$

The quantity tn in Eq. (6) is a single parameter, not the product $t \times n$. Assuming that the amplitudes of the T_e and n_e fluctuations are small compared to the electron temperature and density themselves, the following relation holds:

$$E_{ki} = E_{ki}^0 (1 + \mu_{tt} t^2 + \mu_{tn} tn + \mu_{nn} n^2). \quad (8)$$

The parameters μ_{tt} , μ_{tn} , and μ_{nn} are defined by the formulas

$$\mu_{tt} = \left[\frac{1}{2} \frac{\partial^2 r_{ki}^{\text{eff}}}{\partial T_e^2} (r_{ki}^{\text{eff}})^{-1} T_e^2 \right]_{T_e=\overline{T_e}; n_e=\overline{n_e}}, \quad (9)$$

$$\mu_{tn} = \left[\frac{\partial^2 r_{ki}^{\text{eff}}}{\partial T_e \partial n_e} (r_{ki}^{\text{eff}})^{-1} T_e n_e \right]_{T_e=\overline{T_e}; n_e=\overline{n_e}}, \quad (10)$$

$$\mu_{nn} = \left[\frac{1}{2} \frac{\partial^2 r_{ki}^{\text{eff}}}{\partial n_e^2} (r_{ki}^{\text{eff}})^{-1} n_e^2 \right]_{T_e=\overline{T_e}; n_e=\overline{n_e}}. \quad (11)$$

Our calculations show that the *smallness* can be treated broadly. Even for $t^2 \approx 0.25$ corresponding to the $\pm 50\%$ deviations from the mean temperature, the differences in the total energies emitted by nebulae in optical and ultraviolet lines calculated directly from Eq. (1) and using the approximate relation (8) do not exceed 3–5% in most cases. The same values of the parameters tn and n^2 may also be considered small in the above sense.

The total amplitude of the temperature variations in a nebula is the sum of the large-scale fluctuations related to the relatively slow decrease in mean temperature in the nebula with increasing distance from

its central star and with characteristic sizes comparable to those of the nebula itself and the small-scale fluctuations with sizes much smaller than those of the nebula. According to the calculations by Gruenwald and Viegas (1995), the amplitudes of the large-scale fluctuations are $t_{\text{large-sc}}^2 \leq 0.03$. At the same time, to reconcile the observed and theoretical line intensities in the PNe spectra, $t^2 \approx 0.10\text{--}0.16$ should be used in many cases. Thus, the conclusion that the small-scale fluctuations mainly contribute to the amplitude of the temperature fluctuations suggests itself.

As we see from Eq. (8), the amplitude of the line intensity variations is determined not by the parameter t^2 itself but by the product $\mu_{tt} t^2$. We see from Eq. (9) that the absolute values of the parameter μ_{tt} are low for recombination lines due to the weak temperature dependence of the effective recombination coefficients. For this reason, the recombination line intensities depend weakly on the amplitude of the T_e fluctuations in a nebula.

At the same time, the values of μ_{tt} can be high for collisionally excited lines, since the corresponding effective line formation coefficients increase exponentially rapidly with electron temperature in the line formation region (see, e.g., Kholtygin and Feklistova 1992). For this reason, the intensities of collisionally excited lines can increase by a factor of 2 or more as one passes from a single-temperature nebula to a nebula with the same mean temperature and moderate values of the parameter $t^2 = 0.02\text{--}0.06$.

The intensities of collisionally excited lines depend strongly on the amplitude of the T_e fluctuations; the intensities of recombination lines are barely sensitive to such fluctuations. In the presence of T_e fluctuations, the intensity of the C III $\lambda 1907$ line can increase by a factor of 1.5–2 compared to a homogeneous (in temperature) plasma, while the intensities of the purely recombination H β and C II $\lambda 4267$ lines remain almost constant (Kholtygin 2000).

Present-day observations of planetary nebulae suggest that their chemical composition may vary (Tsamis et al. 2008). Changes in the abundances of C, N, O, and heavier elements in a particular nebular volume cause a change in the cooling rate of the nebular gas, i.e., a change in the gas temperature in this volume. Thus, variations in chemical composition cause the temperature fluctuations in a nebula included in our model to increase. This means that variations in chemical composition with a moderately large amplitude can also be taken into account in our model at least partially.

At the same time, during significant variations in the chemical composition of PNe, their effect is not reduced only to the temperature variations. Therefore, we are planning to introduce an additional parameter

in our model that will describe the variations in chemical composition.

A STOCHASTIC MODEL OF NEBULAE

We use the following semiempirical model (Kholtygin 2000) to take into account the effect of temperature and density fluctuations on the nebular spectra. The nebular region where the lines of the ion group under consideration are formed is a low-density, optically thin (in these lines) plasma. In each plasma volume element, T_e and n_e are random variables characterized by the mean electron temperature $\overline{T_e}$ and density $\overline{n_e}$, their rms fluctuations in this region t^2 and n^2 , and the parameter tn that describes the correlation between the $\overline{T_e}$ and $\overline{n_e}$ fluctuations. We will also assume that the relative elemental abundances are constant in the entire nebular volume.

Generally, each ion X^{n+} present in a nebula is described by its own set of $\overline{T_e} = \overline{T_e}(X^{n+})$ and $t^2(X^{n+})$. However, numerous calculations have shown (e.g., Harrington et al. 1982) that the nebular temperatures averaged over the distribution of ions in PNe are very close. Their values for most of the PNe differ by no more than 100–200 K. The calculations by Gruenwald and Viegas (1995) show that this result does not depend on the model parameters and is retained during variations in the effective temperatures and luminosities of the central stars as well as during variations in the mean electron density and elemental abundances in the nebula.

The values of the parameter t^2 for different ions averaged over the entire nebular volume differ insignificantly. Based on the results of the cited papers, we conclude that the values of $\overline{T_e}$ and t^2 for He^+ , $\text{C}^+ - \text{C}^{4+}$, $\text{N}^{2+} - \text{N}^{3+}$, and $\text{O}^{2+} - \text{O}^{4+}$ are close. In addition, the values of t^2 themselves are determined mainly by small-scale fluctuations whose amplitudes are not too different for different nebular regions. For ions with a lower degree of ionization, O^+ and N^+ , a different set of parameters should be used in the case of highly inhomogeneous nebulae: $\overline{T_e}^*$, $\overline{n_e}^*$, and $(t^2)^*$. The variations in tn and n^2 in PNe can be significant (see, e.g., Rubin 1969). However, since we will consider the nebular emission in lines of elements close in ionization potentials and since the line intensities depend weakly on these parameters, we will also assume the parameters tn and n^2 to be constant in PNe.

In conclusion, we will give a list of model parameters: $\overline{T_e}$, t^2 , $\overline{n_e}$, n^2 , tn , He/H, C/H, N/H, and O/H, where He/H, C/H, N/H, and O/H denote the relative He, C, N, and O abundances: $\text{N}(\text{He})/\text{N}(\text{H})$, $\text{N}(\text{C})/\text{N}(\text{H})$, $\text{N}(\text{N})/\text{N}(\text{H})$, and $\text{N}(\text{O})/\text{N}(\text{H})$, respectively.

Choosing the parameters $\overline{T_e}$ and t^2 for the H II and He II regions is a special question. Since the volume of these regions can exceed that of the C III–V, N III–IV, and O III–V regions, the values of $\overline{T_e}(\text{H II})$ and $\overline{T_e}(\text{He II})$ should be lower than those for the above ionization regions. At the same time, these differences are not very large and do not exceed 1000–1500 K (Harrington et al. 1982); when these differences are taken into account, the hydrogen and helium line intensities (averaged over the entire volume of the H II or He II regions) change by no more than 2–3%, which is smaller than the measurement errors of the observed line fluxes. For this reason, we will use the model parameters adopted for the C III–V, N III–IV, and O III–V regions to calculate the H I and He I line intensities.

An iterative procedure for reconciling the observed and calculated line intensities is a standard method for determining the nebular parameters. The result of this procedure depends in an obvious way on the adopted fitting method and the accuracy of the data used. It is important to note that the line intensities in the nebular spectra are measured with an error that depends significantly on the line intensity itself. Whereas the measurement error in the intensities of strong lines does not exceed 5% (Feibelman et al. 1996), the measurement error in the intensities of weak lines (whose intensity is less than 0.01 of the $\text{H}\beta$ line intensity) can be 30–50% or more. This circumstance is usually disregarded when the nebular parameters are determined. To take into account the different measurement accuracies of the line intensities, Kholtygin (1998a) suggested a procedure based on the principle of maximum likelihood (see, e.g., Brandt 1975). We also used the same procedure here. We will call the nebular parameters determined using this procedure *optimal* ones.

Following Kholtygin (1998a), we will assume that a normal law can be used for the intensity distribution function of strong lines:

$$P^N(I) = \frac{1}{\sigma^N \sqrt{2\pi}} \exp \left[-\frac{1}{2} \left(\frac{I^{\text{obs}} - I}{\sigma^N} \right)^2 \right], \quad (12)$$

where I is the mean value of the observed line intensity, I^{obs} is the observed value of the line intensity, and we will use the following approximate relation for the standard deviation σ^N :

$$\sigma^N = \alpha \sqrt{I^{\text{obs}} I (N_1 + N_2)}, \quad (13)$$

which is based on the analysis of a large number of observations of nebular spectra (Rola and Stasinska 1994). Here, $I(N_1 + N_2)$ is the total intensity of the nebular $[\text{O III}](4959 + 5007)$ Å lines in the nebular spectrum. The values of the parameter $\alpha \approx$

Table 1. Intensities of ultraviolet and optical lines in the spectrum of NGC 5882

Species	λ , Å	I^{obs}	I^{calc}	$\frac{ I^{\text{obs}} - I^{\text{calc}} }{\sigma(I^{\text{obs}})}$	$\sigma(I^{\text{obs}})$
He	5876	16.00	15.51	0.41	1.20
He	6678	4.31	4.74	0.69	0.62
He ⁺	4686	2.75	2.75	0.00	0.50
C ⁺	4267	0.40	0.09	1.64	0.19
C ²⁺	1907	24.70	25.31	0.14	4.47
C ²⁺	4650	0.06	0.06	0.00	0.07
N ⁺	5755	0.27	0.16	0.68	0.16
N ⁺	6548	4.87	4.90	0.05	0.66
N ⁺	6583	14.40	14.43	0.03	1.14
N ²⁺	1750	4.50	4.50	0.00	1.91
N ²⁺	4640	1.12	1.12	0.00	0.32
O ⁺	3726	10.20	8.81	1.45	0.96
O ⁺	3729	4.98	5.98	1.49	0.67
O ²⁺	1663	4.90	5.24	0.17	1.99
O ²⁺	4363	5.56	5.65	0.12	0.71
O ²⁺	4931	0.14	0.10	0.32	0.11
O ²⁺	4959	353.0	361.7	1.54	5.64
O ²⁺	5007	1050.0	1040.8	0.94	9.72

0.01 for optical and infrared lines and $\alpha \approx 0.03$ for ultraviolet lines.

As the line intensity decreases, its relative measurement error increases. For weak lines ($I^{\text{obs}} < 0.1$ on the scale $I(\text{H}\beta) = 100$), we used a lognormal distribution with a shift that was suggested by Rola and Pelat (1994) and that describes the systematic overestimation of the observed intensities of weak lines to describe the line intensity distribution function.

Table 1 presents typical results of reconciling the observed and calculated intensities of optical and ultraviolet lines in the spectrum of the nebula NGC 5882. The observed line intensities in the nebular spectrum were taken from Tsamis et al. (2003). The first two columns in Table 1 list the ions and wavelengths in Å; the third and fourth columns list the observed (corrected for the interstellar reddening) and calculated line intensities. The next column lists the absolute values of the differences between the observed and calculated intensities in units of the standard deviation calculated from Eq. (13) for the intensity distribution function (12) given in the last column of Table 1. From the table, we see a good

Table 2. Comparison of the observed (I^{obs}) infrared CII and OIII line intensities in the spectra of the nebulae NGC 3918, NGC 6543, and NGC 6572 with the calculated ones (I^{calc}) in the stochastic models of nebulae

Ion	λ , μm	I^{obs}	I^{calc}	Elemental abundance [X] = $\log(N(X)/N(\text{H})) + 12$	
				without IR lines	with IR lines
NGC 3918					
C ⁺	157	0.21	0.21	8.57	8.64
O ²⁺	52	88.6	83.4	9.06	8.57
	88	27.5	31.8		
NGC 6543					
C ⁺	157	0.18	0.18	8.39	8.37
O ²⁺	52	208.17	216.7	8.30	9.01
	88	60.70	49.94		
NGC 6572					
C ⁺	157	0.46	0.46	9.03	8.86
O ²⁺	52	40.6	40.8	9.16	9.11
	88	6.61	4.49		

quality of the fit to the observed nebular spectrum in the stochastic model.

When the total abundances of He, C, N, and O atoms are determined from the abundances of their individual ions, the ionization corrections for the unobservable ionization stages should be applied. The abundance of ion X^{m+} of element X can be derived from the relation

$$N(X^{m+}) = r(X^{m+})N(X),$$

where $r(X^{m+})$ is the relative abundance of ion X^{m+} in the total abundance $N(X)$ of element X.

The relative ion abundance is usually determined by constructing ionization models of nebulae. Our analysis (see, Kholtygin 1998a) shows that this value is characterized mainly by the nebular excitation class E_x (Aller and Liller 1966). Using the results of numerous calculations of ionization models for nebulae from Aller and Czyzak (1979, 1983), we obtained the dependences of $r(X^{m+})$ averaged over the nebular excitation class on E_x for C, N, and O ions. The values of $r(X^{m+})$ found for carbon ions turned out to be close to their empirical values obtained by Kholtygin (1984) by studying the recombination lines of carbon ions.

For the ions under considerations and nebulae of any excitation classes, the ionization corrections for

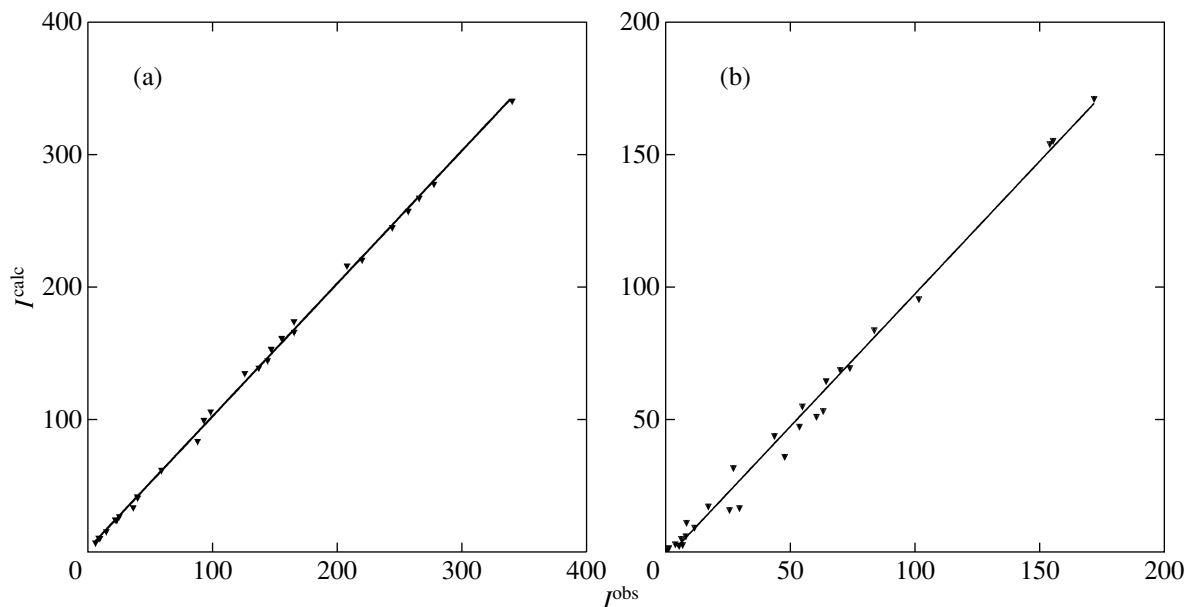


Fig. 1. Comparison of the observed and calculated intensities of the infrared O III λ 52 μm (a) and O III λ 88 μm (b) lines in the PNe spectra.

the ionization stages whose lines are absent in the nebular spectra are less than two. Our analysis of the possible errors in E_x and the related errors in the factors $r(X^{m+})$ leads us to conclude that the errors in the total C, N, and O abundances do not exceed 10–20%. To find the excitation class E_x of the nebulae, we used the line intensity ratios for elements of different ionization stages in the nebular spectra according to the criteria from Aller and Liller (1966) and Gurzadyan (1962).

In the last decade, with the launch of the ISO and Spitzer infrared telescopes, it has become possible to use the intensities of the infrared lines of transitions between the fine-structure levels of C, N, O, and other elements to analyze the PN spectra. Comparison of the intensities of the infrared C⁺ and O²⁺ lines in Table 2 calculated in our stochastic model for three bright planetary nebulae with the observed ones from Liu et al. (2001) leads us to conclude that this model describes faithfully the infrared nebular spectrum. This conclusion is illustrated in Fig. 1, in which we see good agreement of the observed infrared O III line intensities with those calculated in the stochastic model. At the same time, as we see from Table 2, excluding the infrared lines from the list of lines used to construct the nebular models can lead to significant errors in the elemental abundances in the nebulae in several cases.

PARAMETERS OF GALACTIC PLANETARY NEBULAE AND THEIR ERRORS

Table 3 gives the nebular parameters and the helium, carbon, nitrogen, and oxygen abundances that

we derived. The sources of the line intensities used to determine the nebular parameters are presented on the page http://www.astro.spbu.ru/staff/afk/GalChemEvol/Neb_Ab.html at the site of the Astronomical Institute of the St. Petersburg State University.

To calculate r_{ki}^{eff} , the effective formation coefficients of collisionally excited lines, we solved the level population balance equations for all of the C, N, and O ions whose lines were present in the nebular spectra. The necessary atomic data and r_{ki}^{eff} for recombination lines were taken either from the catalog by Golovatyj et al. (1997) or from the papers cited by Bychkov and Kholtygin (2007).

Columns 1 and 2 in Table 3 give the PN name and excitation class E_x . Column 3 contains the electron temperature T_e and column 4 gives the parameter t^2 that describes the amplitude of the rms fluctuations in T_e . Column 5 contains the electron density used in our calculations. Columns 6–9 present the derived He, C, N, and O abundances on a logarithmic scale: $[X] = \log(N(X)/N(\text{H})) + 12$. Since the dependence of the line intensities in the nebular spectra on n^2 and tn is weak, their values cannot be determined with a sufficient accuracy and they are not given in the table. The nebula NGC 7027 for which the parameters n^2 and tn are given in Kholtygin (2000) constitutes an exception.

The errors of the nebular parameters in our stochastic model are determined by the inaccuracies in measuring the observed line intensities, the errors

Table 3. He, C, N, and O abundances in Galactic planetary nebulae

PN	Ex	$\overline{T_e}$	t^2	n_e	$[X] = \log(N(X)/N(H)) + 12$			
					[He]	[C]	[N]	[O]
A12	5	11430	0.000	2.60×10^2	11.10		8.23	8.42
A18	5	15400	0.000	3.60×10^2	11.12		8.21	7.91
A20	6	10680	0.000	9.87×10^3	10.93		8.46	8.15
BB1	4	12920	0.000	4.09×10^3	10.99	8.96	8.11	7.74
BD + 3036	2	9350	0.000	1.30×10^3	10.44	8.61	7.96	8.58
BoBn1	4	8690	0.000	4.20×10^4	11.11		7.48	8.49
DdDm1	4	12260	0.034	7.36×10^3	11.04	7.18	7.99	8.07
H3-75	6	12730	0.000	1.20×10^2	10.90		8.23	8.62
H4-1	4	11990	0.036	8.82×10^2	11.08	9.19	7.55	8.41
Hb4	6	9520	0.000	5.88×10^3	11.18	9.51	8.43	8.67
Hb12	4	11060	0.000	5.22×10^5	11.03	8.55	8.14	7.65
Hu1-2	10	19520	0.000	2.12×10^3	11.09	8.21	8.19	8.01
Hu2-1	4	6580	0.103	1.07×10^4	11.11	8.89	8.49	8.49
IC2003	8	11950	0.000	5.14×10^3	11.03	8.21	7.65	8.59
IC2165	8	9340	0.120	2.82×10^3	11.04	9.17	9.08	8.92
IC2448	7	13100	0.000	1.19×10^2	11.12			8.44
IC3568	5	10900	0.000	1.08×10^3	11.01	8.61	8.16	8.34
IC4191	5	6450	0.108	9.65×10^3	11.21	8.96	8.99	9.01
IC4406	5	10070	0.000	4.81×10^2	11.08	8.39	8.60	8.63
IC4593	3	6000	0.076	8.28×10^2	11.12	8.76	8.87	8.66
IC5117	6	16840	0.000	1.09×10^4	11.33	8.65	8.56	7.58
IC5217	6	7250	0.101	1.25×10^4	11.14	8.73	9.05	8.95
J320	5	8220	0.120	4.30×10^3	11.17		8.65	8.87
J900	7	7440	0.100	4.77×10^3	11.04	9.15	9.10	8.98
K1-7	6	15750	0.000	36.8	11.06		8.22	8.03
K2-1	8	6030	0.130	7.36×10^3	10.91		8.38	8.88
K3-66	3	6050	0.100	2.39×10^4	11.09		7.78	8.25
K3-70	6	15220	0.000	3.05	11.18		8.72	7.87
K648	4	10710	0.044	4.44×10^3	11.00	9.13	7.87	7.92
M1-6	3	6760	0.100	1.22×10^4	11.04		7.97	8.20
M1-7	5	9430	0.000	2.53×10^4	11.17		8.46	8.63
M1-8	7	16140	0.000	1.30×10^2	11.17		8.92	8.20
M1-9	5	10700	0.000	1.03×10^4	10.89		7.86	8.23
M1-13	6	6010	0.080	1.13×10^3	11.24		8.63	9.00
M1-14	3	11220	0.090	1.93×10^3	11.01		7.18	8.09
M1-16	7	6810	0.080	6.73×10^3	11.21		10.10	9.35
M1-17	7	6550	0.090	4.80×10^3	11.06		9.49	9.15
M1-18	4	7840	0.006	4.09×10^4	11.26		8.76	9.03
M1-25	4	7460	0.000	1.29×10^4	11.25	8.86	10.00	9.03
M1-50	7	6840	0.099	6.09×10^3	11.15		9.40	9.21
M1-54	6	10420	0.000	3.84×10^3	11.19	8.95	9.36	8.61
M1-57	7	7530	0.100	1.02×10^4	11.17	9.56	9.32	9.20
M1-74	5	6150	0.100	2.60×10^4	11.17	9.05	7.91	9.31
M1-80	6	6710	0.080	1.10×10^2	11.07	9.17	9.12	9.03
M3-2	7	13200	0.000	2.02×10^3	11.43		9.49	8.09
M3-15	5	8420	0.000	3.70×10^3	11.18	8.55	9.25	8.93
Me1-1	5	6790	0.100	5.03×10^3	11.19	7.74	8.87	8.98

Table 3. (Contd.)

PN	Ex	\bar{T}_e	t^2	n_e	$[X] = \log(N(X)/N(H)) + 12$			
					[He]	[C]	[N]	[O]
MyCn18	4	8980	0.100	2.47×10^3	11.09	8.64	8.27	8.25
Mz1	6	7450	0.000	5.38×10^3	11.43	8.73	11.54	8.47
NGC40	2	8510	0.000	2.09×10^3	10.87	8.45	7.96	8.61
NGC650A	5	11160	0.036	4.68×10^2	11.01	9.02	8.25	8.49
NGC650B	5	11150	0.027	4.68×10^2	11.02	9.02	8.55	8.57
NGC1514	5	14550	0.000	15.2	10.97		7.51	8.25
NGC1535	7	7480	0.108	1.51×10^4	10.93	8.18	8.85	8.70
NGC2371	9	8540	0.094	2.00×10^3	11.03	8.57	8.93	8.90
NGC2438	7	9090	0.049	1.09×10^4	11.08	9.46	9.18	9.12
NGC2440	9	11780	0.062	4.24×10^3	11.10	8.96	9.15	8.94
NGC3132	6	9680	0.062	3.74×10^2	11.12	8.45	8.26	8.60
NGC3242	6	14020	0.093	7.98×10^2	11.02	8.01	8.30	8.27
NGC3587	5	10810	0.000	6.84×10^3	10.93		7.96	8.64
NGC3918	9	12510	0.061	4.05×10^3	11.05	8.65	8.23	8.71
NGC2818	6	14430	0.060	9.92×10^2	11.13	8.22	8.74	8.28
NGC5307	5	8350	0.072	1.95×10^4	11.08	8.25	8.37	8.98
NGC5315	4	6040	0.126	9.93×10^3	11.23	5.83	8.04	8.67
NGC5882	9	9470	0.000	2.68×10^3	11.10	8.14	8.60	8.91
NGC6072	7	9670	0.000	1.13×10^4	11.40		9.66	8.93
NGC6153	6	7030	0.048	2.12×10^3	11.24	8.09	8.73	8.92
NGC6210	5	7680	0.025	3.62×10^3	11.07	8.27	8.31	8.99
NGC6302	9	6970	0.128	3.53×10^4	11.35	9.47	9.87	10.22
NGC6309	8	10220	0.072	30.6	11.11	9.21	9.12	8.77
NGC6369	5	6530	0.090	4.05×10^3	11.16		8.35	9.08
NGC6543	5	7860	0.000	3.26×10^3	11.26	8.71	8.29	8.96
NGC6567	5	10840	0.024	1.27×10^4	11.07	8.94	8.72	8.45
NGC6572	6	8900	0.119	1.79×10^4	11.17	8.12	8.23	8.86
NGC6578	6	6000	0.097	9.39×10^2	11.20	9.49	9.33	8.78
NGC6720	6	10430	0.000	3.79×10^2	11.05	8.78	8.64	8.58
NGC6741	8	13400	0.082	6.35×10^3	11.09	8.49	8.29	8.50
NGC6781	7	10890	0.000	5.29×10^2	11.10	9.37	9.18	8.68
NGC6790	6	14090	0.000	2.67×10^4	11.08	8.24	8.09	8.30
NGC6818	6	11840	0.104	3.08×10^3	11.03	8.42	8.08	8.61
NGC6826	5	8330	0.078	7.83×10^2	11.08	8.20	8.13	8.45
NGC6833	5	10740	0.059	6.73×10^4	11.16		7.57	8.47
NGC6879	5	9130	0.024	2.60×10^4	11.10		9.00	8.72
NGC6884	6	9600	0.081	5.15×10^3	11.06	8.47	8.75	8.34
NGC6886	8	11050	0.031	7.57×10^3	11.12	8.82	8.61	8.79
NGC6891	5	9520	0.000	2.95×10^3	11.08	8.85	8.84	8.51
NGC6894	5	7180	0.000	2.99×10^4	11.14		8.82	9.10
NGC6905	7	11740	0.000	2.51×10^2	11.01	8.69	7.28	8.57
NGC7009	6	6510	0.098	3.60×10^3	11.17	9.22	9.23	8.94
NGC7026	6	7600	0.015	7.22×10^3	11.19	9.38	9.33	9.05
NGC7027	10	12100	0.037	5.18×10^4	11.08	8.92	8.44	8.92
NGC7662	8	12270	0.057	1.83×10^3	11.03	8.90	7.76	8.61
SwSt1	3	7500	0.070	1.62×10^4	10.73	7.91	7.90	8.18
Tc1	5	9610	0.000	1.26×10^3	10.87	8.59	8.00	8.09

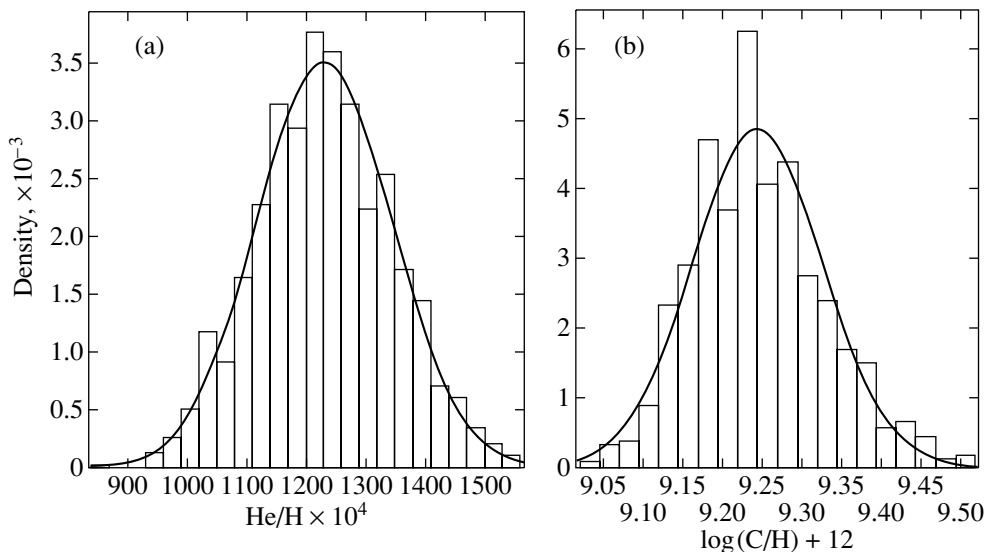


Fig. 2. (a) Error distribution function for the He abundance in NGC 7027 (on a linear scale) and its Gaussian fit (solid line). (b) The same as Fig. 2a for the carbon abundance (on a logarithmic scale).

of the ionization corrections (when the elemental abundances are derived), and the inaccuracies in the atomic data.

The errors of the elemental abundances related to the inaccuracies in the ionization corrections were considered in the previous section and do not exceed 0.06 dex. The contribution from the inaccuracies in the atomic data to the total errors in the elemental abundances is also small, since present-day calculations show that the errors in the transition probabilities and collision strengths for forbidden, intercombination, and permitted lines used to calculate the line intensities in the PNe spectra do not exceed 5–10% in most cases (Niimura et al. 2002).

Thus, we conclude that the errors in the nebular parameters are attributable mainly to the inaccuracies in the observed line intensities. In this section, we investigate the effect of intensity measurement errors on the global characteristics of PNe determined from these intensities. We used a stochastic simulation procedure to analyze the errors in the PNe parameters. Since the line fluxes being measured in the nebular spectra are random variables, the quantities being analyzed, the line intensities, are also random variables.

For our simulations, we chose the nebula NGC 7027. Since the observed line intensities in its spectrum are known with a high accuracy, to a first approximation, they may be assumed to be equal to their expectation values. Suppose that $n \gg 1$ determinations of line intensities in the nebular spectrum were made. For the random variable I_k , the line intensity in the nebular spectrum, where k is the measurement number, we can assume the

normal distribution (12) whose standard deviation σ^N will be described by Eq. (13) to be valid. As the vector of expectation values for the line intensities, we will take the set of intensities determined by Zhang et al. (2005) from highly accurate line flux measurements in the nebular spectrum.

We obtained a sample of $n = 1000$ values of the random vectors of line intensities in the nebular spectrum with the distribution function (12) by the standard methods of statistical simulations. The nebular parameters were determined from each of the vectors of this sample using the procedure described above. The nebular parameters obtained from our simulations are also random variables. Since the nebular parameters depend nonlinearly on the line intensities, their distribution function will not necessarily be normal and should be established from an additional analysis.

Since the abundance of an element in a nebula is proportional to the intensities of the ion lines of this element in the nebular spectrum, to a first approximation, the hypothesis that the distribution of elemental abundances is normal may be assumed to be valid. We tested the hypothesis that the distribution of the derived elemental abundances in NGC 7027 is normal using the χ^2 test (Brandt 1975) at the significance level $\alpha = 10^{-3}$.

Our analysis shows that only the helium abundance distribution satisfies the normality criterion. The resulting distribution functions of the He/H abundance ratio (on a linear scale) and the carbon abundance (on a logarithmic scale) are presented in Figs. 2a and 2b, respectively.

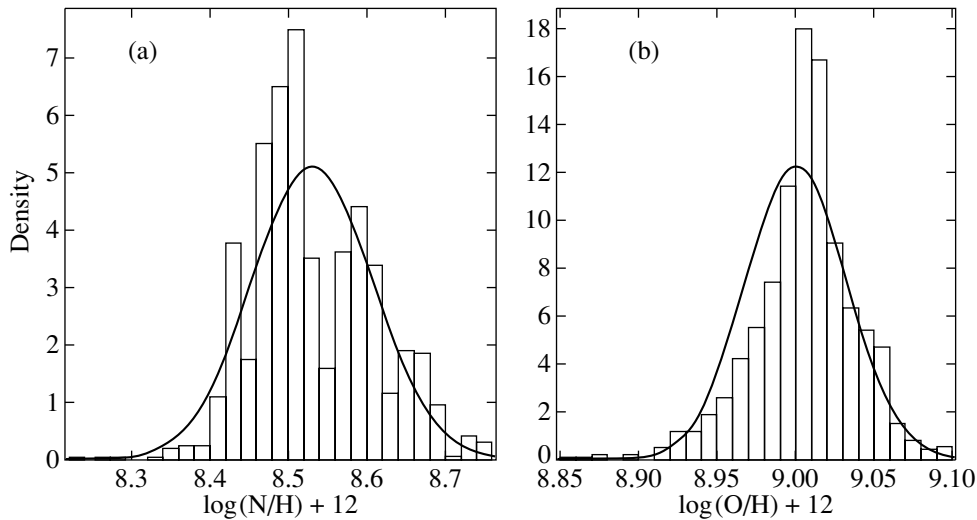


Fig. 3. Same as Fig. 2 for the N (a) and O (b) abundances.

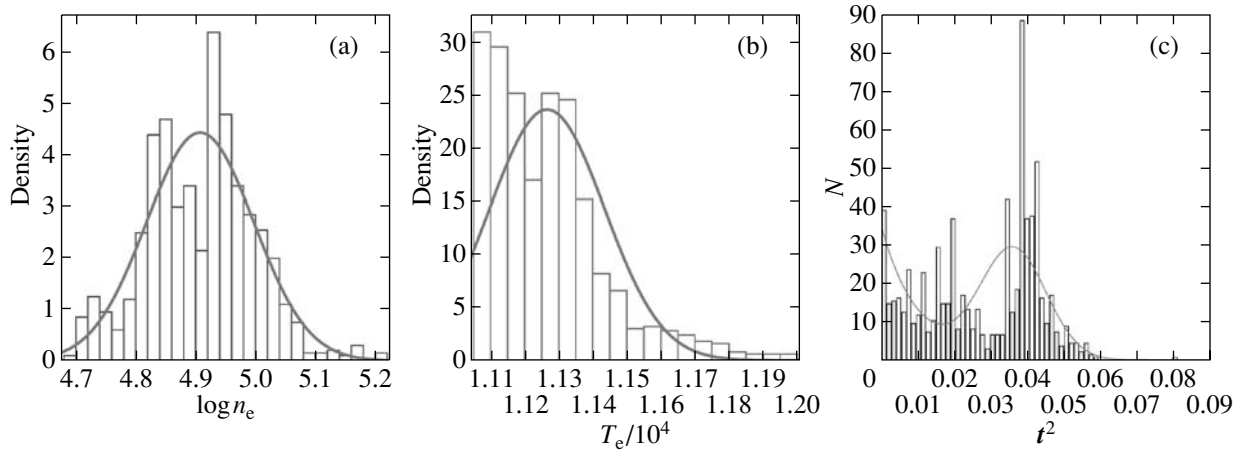


Fig. 4. Same as Fig. 2 for $\log n_e$ (a), T_e (b), and the parameter t^2 (c). The dashed line represents the fit to the t^2 distribution function by the sum of exponential and normal distributions (see the text).

This result can be easily explained. The He abundance in a nebula is determined from the intensities of recombination lines, which depend weakly on the mean nebular electron temperature and the amplitude of its fluctuations. At the same time, the intensities of the *collisionally excited* lines of CNO ions depend exponentially on the temperature; the exponents are determined by the level structure of the specific ion and can differ greatly for different lines of the same ion as well as for the lines different ions.

The aforesaid is illustrated in Fig. 3, which presents the inferred N and O abundance distribution functions on a logarithmic scale. We see a significant asymmetry of the distribution functions. It may be concluded from our analysis that the He abundance is determined with an accuracy of about 10–15%, while the errors in the derived C, N, and O abundances

are 0.1–0.2 dex. Including the inaccuracies in the ionization corrections for the ionization stages of the elements whose lines are absent in the nebular spectra increases the errors in the He abundance to 0.1 dex and in the C, N, and O abundances to 0.3 dex.

Figure 4 presents the distribution functions of the logarithm of electron density n_e , electron temperature $T_e/10^4$, and t^2 . The errors in the electron temperature do not exceed 100–200 K, while the errors in n_e are 10–20%. The t^2 distribution function can be represented by the sum of two components. The first and the second can be described by exponential, $f_{\text{exp}}(t^2) = 35 \exp(-0.01t^2)$, and normal, $f_{\text{norm}}(t^2) = 29 \exp\{-[0.5(t^2 - 0.036)/0.009]^2\}$, distribution functions. The contribution from the exponential and normal distribution components to the total distribution functions is 35 and 65%, respectively.

Table 4. Modified (Quireza et al. 2007) classification of Galactic PNe according to Peimbert (1978)

Type	He/H	lg(N/O)	log(N/H) + 12	\overline{M} , M_{\odot}	\overline{z} , kpc	Galactic region
I	≥ 0.125	≥ -0.30	—	0.64–1.09	$\ll 1 (< 0.3)$	Thin disk
II	IIa ≥ 0.125	< -0.30	≥ 8.00	0.57–0.64	< 1	Thin disk
	IIa < 0.125	≥ -0.60	≥ 8.00			
	IIb < 0.125	< -0.60	< 8.00			
III	—	—	—	0.56–0.57	$\geq 1 (< 1.45)$	Thick disk
IV	—	—	—	0.55–0.56	$\gg 1 (> 1.45)$	Halo
V	—	—	—	Large spread	< 1.3	Bulge

Table 5. Global parameters of PNe in our Galaxy and the Magellanic Clouds

Type	\overline{z} , kpc	$\sigma_{\overline{z}}$	\overline{M} , M_{\odot}	σ_M	Element [X] = log(X/H) + 12							
					$\overline{[He]}$	$\sigma_{[He]}$	$\overline{[C]}$	$\sigma_{[C]}$	$\overline{[N]}$	$\sigma_{[N]}$	$\overline{[O]}$	$\sigma_{[O]}$
I	0.23	0.25	0.686	0.081	11.21	0.1	8.32	1.35	8.96	0.66	8.63	0.69
IIa	0.31	0.29	0.638	0.046	11.13	0.09	8.82	0.44	8.73	0.69	8.75	0.33
IIb	0.56	0.36	0.617	0.033	11.03	0.1	8.55	0.4	8.36	0.57	8.53	0.38
III	1.05	1.12	0.599	0.026	10.94	0.27	8.60	0.01	7.92	0.50	8.41	0.30
IV	1.35	0.0	0.588	0.0	11.06	0.06	8.64	0.84	7.98	0.5	8.22	0.36
Bulge	0.56	0.29	0.614	0.03	11.16	0.1	8.74	0.44	8.59	0.59	8.86	0.42
LMC	—	—	—	—	11.02	0.11	8.8	0.58	7.49	0.86	8.24	0.55
SMC	—	—	—	—	11.10	0.08	8.98	0.83	8.08	1.03	8.30	0.21

The derived dependence can be explained as follows. The first and second components correspond, respectively, to the contributions from the small-scale and large-scale T_e fluctuations in the nebula. To reach a more reliable conclusion about the contribution from temperature variations of different nature to the total amplitude of the T_e fluctuations, the t^2 distribution function should be investigated for other PNe.

AN ENSEMBLE OF PLANETARY NEBULAE OF OUR GALAXY AND THE MAGELLANIC CLOUDS

The characteristics of PNe depend mainly on the masses of their progenitor stars, which differ greatly for objects of different Galactic subsystems. Conclusions about the origin of PNe in various Galactic subsystems and the Magellanic Clouds can be reached by comparing their characteristics.

It is most convenient to use the classification of PNe by Peimbert (1978), whose criteria (in a version modified by Quireza et al. (2007)) are presented in Table 4, to determine which Galactic subsystem a particular nebula belongs to. Type I nebulae correspond

to initial masses of their main-sequence progenitor stars $M_{\text{ini}} \geq 2.4M_{\odot}$, while type II and III nebulae correspond to $M_{\text{ini}} \leq 2.4M_{\odot}$.

The last columns in Table 4 give the mean masses of the central stars of these types \overline{M} and their mean heights above the Galactic plane \overline{z} . To pass from the masses of the progenitor stars to those of the central stars of PNe, we used the initial mass–final mass for intermediate-mass stars (Milanova and Kholtygin 2006).

The difference between the mean parameters of type I–V nebulae is illustrated in Table 5, which presents the mean heights of nebulae of various types above the Galactic plane \overline{z} that we calculated using our data and those from the catalog by Kholtygin and Milanova (2008), the mean masses of their central stars \overline{M} , the mean elemental abundances [X], and the standard deviations σ_z , σ_M , and $\sigma_{[X]}$ of these quantities. The values of \overline{z} increase regularly, while the values of \overline{M} decrease as we pass from type I to type IV nebulae.

We see from Table 5 that type I nebulae differ from those of other types by the larger mean mass of their central stars and by their higher concentration toward the Galactic plane. The differences in the mean masses of type II and III nebulae are statistically insignificant, while the mean height of nebulae above the Galactic plane increases significantly as we pass from subtype IIa to type III.

According to the data in Table 5, the mean oxygen abundance in the LMC is slightly (by 0.06 dex) lower than that in the SMC, although the O abundance for other objects (stars, giant H II regions) is higher in the LMC. Recently, Wang and Liu (2008) obtained the mean abundance $[O/H] = 8.38$ for an ensemble of PNe in the LMC, which is higher than our value by only 0.14 dex, while for SMC nebulae, they obtained $[O/H] = 8.10$, which is lower than our value of 8.30 by 0.20 dex. Thus, we found the mean $[O]$ in the LMC to be lower than that in the SMC, most likely due to the random deviation in opposite directions from the mean value for all LMC and SMC nebulae, respectively.

One of the most important, as yet unsolved questions in the physics of our Galaxy is the origin of its bulge. The bulges are separated into “true” bulges formed in S0–Sb spiral galaxies through the accumulation of the gaseous or stellar component of the galaxies at early phases of their evolution and “pseudobulges” formed in late-type spiral galaxies due to the instability of their disks. The bulge of our Galaxy is most likely a “true” one (Zoccali et al. 2006; Matteucci 2008).

The following scenarios are most often suggested for the formation of true bulges: accretion of the already formed stellar aggregates at the galactic center; accumulation of the gas located in the central regions of the galaxy during its formation, resulting in star formation and the formation of the stellar component of the bulge; accretion of a metal-rich gas in the halo and the thin and thick disks (Matteucci 2008).

According to Zoccali et al. (2006), the bulge formation through the mergers of rapidly moving massive molecular clouds in the central Galactic region and the subsequent starbursts resulting from these mergers is the most likely scenario suggested by Immeli et al. (2004). The same conclusion was reached in the review by Minniti and Zoccali (2007), in which the bulge is said to have been rapidly formed during the first billion years of Galactic evolution.

However, even if this scenario is valid for our Galaxy, many details of the bulge formation and its role in various Galactic subsystems, in particular, the thin and thick disks, remain unclear. Analysis of elemental abundances in these subsystems can shed light on this question. Meléndez et al. (2008)

determined the C, N, O, and Fe abundances in the atmospheres of red giants in the Galactic disk and bulge and concluded that the abundances of these elements are similar in bulge and thick-disk objects.

Note, however, that analysis of Figs. 2 and 3 from Meléndez et al. (2008), which present the dependences of the $[O/Fe]$ and $[C+N/Fe]$ abundance ratios on metallicity $[Fe/H]$, in our opinion, does not allow one to conclude that the difference between these ratios for thin- and thick-disk objects is statistically significant. Based only on the data from Meléndez et al. (2008), we can conclude that these abundances are similar in bulge and thin-disk objects with the same degree of confidence.

Gutenkunst et al. (2008) concluded that the O, Ne, Ar, and S abundances in bulge and thin-disk PNe differ significantly. This conclusion is in conflict with our analysis of the mean elemental abundances in PNe of various types whose results are presented in Table 5.

The conclusion reached by Gutenkunst et al. (2008) is based on an analysis of *all* disk nebulae, while the elemental abundances depend on the age of the progenitor stars of PNe (see, e.g., Luneva and Kholtygin 2002). To ascertain which PNe belonging to the Galactic disk are similar to bulge objects, we compared the He, C, N, and O abundances in bulge and disk nebulae. Our analysis shows that the bulge nebulae and type II PNe are most similar in the abundances of these elements. The thin-disk type IIa nebulae are most similar in He and CNO abundances in bulge PNe, as illustrated in Fig. 5a.

Besides, as we see from the data in Table 5, the mean heights \bar{z} of thin-disk (Peimbert type III) nebulae above the Galactic plane exceed significantly the values of \bar{z} for bulge PNe and exceed the bulge sizes in the plane perpendicular to the Galactic disk (Minniti and Zoccali 2007). At the same time, the mean heights \bar{z} of type II and bulge nebulae are in much better agreement.

According to the data in Table 4, the type IIa nebulae are thin-disk objects and correspond to an intermediate age of their progenitor stars equal to 4–6 Gyr from the present epoch (Quireza et al. 2007). The similarity of bulge and thin-disk PNe suggests that intense star formation in the bulge, as in the thin disk, took place at least before an epoch no more than 4–6 Gyr away from the present one.

If our conclusion is valid, then the dependence of elemental abundances in PNe on the Galactocentric distance R should continue a similar dependence for thin-disk PNe. To test this assumption, we analyzed the R dependence of the O abundance. Since the O abundance is almost constant during the evolution of intermediate-mass stars, its value in PNe reflects

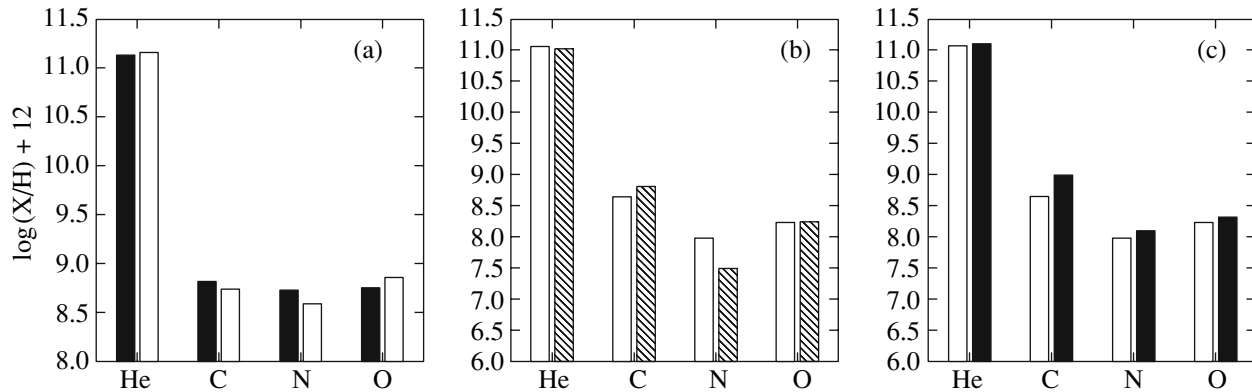


Fig. 5. Comparison of the He, C, N, and O abundances in PNe of various Galactic subsystems: (a) Galactic type IIa PNe (dark columns) and bulge nebulae (light columns); (b) the same as Fig. 5a for PNe of the Galactic halo and the LMC; (c) the same as Fig. 5b for SMC nebulae.

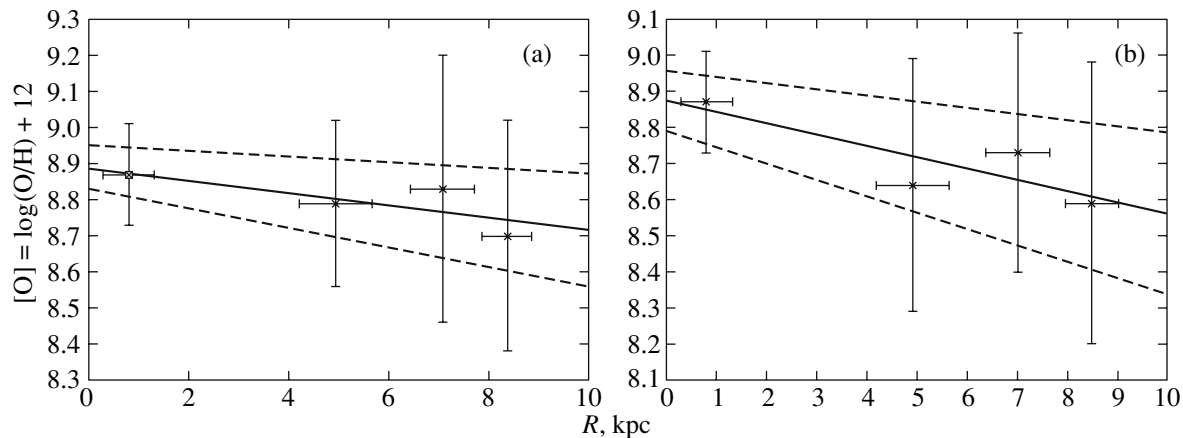


Fig. 6. (a) Dependence of the averaged oxygen abundances in type IIa (asterisks) and bulge (filled squares) nebulae on their mean Galactocentric distance: the solid line represents a linear fit to this dependence with a slope equal to the gradient $d[\text{O}/\text{H}]/dR$; the dotted lines represent the same fit with slopes differing by ± 1 standard deviation of $d[\text{O}/\text{H}]/dR$. (b) The same as Fig. 6a for all type II nebulae.

the primordial O abundance in their progenitor stars determined by the abundance of oxygen in the interstellar medium at the time of their formation.

In finding this dependence, we represented the Galactic disk by a system of five nested rings with the width $\Delta R = 2$ kpc from the Galactic center to $R = 10$ kpc. We assigned the objects within the first ring with Galactocentric distances less than 2 kpc that were classified by Quireza et al. (2007) as bulge nebulae to the bulge PNe.

The question of whether the type II PNe located within the second ring ($2 \text{ kpc} \leq R \leq 4 \text{ kpc}$) belong to the bulge or the disk is not quite clear. On the one hand, since the bulge extent in the Galactic plane does not exceed ± 2 kpc from the Galactic center (see, e.g., Minniti and Zoccali 2007), the nebulae in this region should belong to the disk. On the other hand, according to Quireza et al. (2007), some of

the PNe located at Galactocentric distances of 2–4 kpc are considered to belong to the bulge, which seems doubtful. These nebulae may belong not to the bulge but to the bar or the disk. However, it should be noted that they can actually be bulge objects whose Galactocentric distances were overestimated due to the underestimation of the PNe distances from the Sun in the currently existing PNe distance scales pointed out by Nikiforov and Bobrova (1999).

Since the status of the objects whose Galactocentric distances are within the second ring is uncertain, we excluded them from the general sample of thin-disk and bulge PNe. All of the type II nebulae located at Galactocentric distances $R \geq 4$ kpc were considered to belong to the thin disk. For all of the bulge or disk nebulae with Galactocentric distances within the ring, we determined the mean O abundances and the corresponding standard deviations. These abun-

Table 6. He, C, N, and O abundances in PNe of the Magellanic Clouds. The columns of the table are described in the heading of Table 3

PN	Ex	T_0	t^2	n_e	$\log(N(X)/N(H)) + 12$			
					[He]	[C]	[N]	[O]
LMC-SMP1	4	7187	0.100	1.92×10^4	11.09	9.15	8.04	8.76
LMC-SMP2	3	8763	0.080	5.98×10^2	11.04	8.14	6.96	8.15
LMC-SMP3	4	13428	0.000	2.03×10^4	10.90		6.19	7.73
LMC-SMP4	8	10369	0.000	1.07×10^5	11.13		9.07	8.91
LMC-SMP5	3	13717	0.040	50.3	10.80		6.14	7.81
LMC-SMP6	6	11200	0.090	4.53×10^3	10.96		8.06	8.75
LMC-SMP7	8	20983	0.023	1.11×10^3	10.97		7.76	7.78
LMC-SMP8	4	8414	0.000	2.77×10^5	11.25		6.76	8.14
LMC-SMP9	6	15366	0.000	2.37×10^3	11.04		7.97	8.06
LMC-SMP10	5	13102	0.100	3.53×10^4	10.99		7.57	8.90
LMC-SMP11	3	29164	0.000	2.84×10^3	10.95		6.64	6.97
LMC-SMP61	5	9361	0.014	1.78×10^4	11.11	9.41	7.32	8.70
LMC-N141	5	10252	0.000	5.04×10^4	11.07	8.49	7.81	8.45
LMC-N66	7	14753	0.035	1.95×10^3	11.01		8.51	8.23
SMC-SMP1	4	11235	0.000	5.03×10^4	10.97	8.59	6.98	8.12
SMC-SMP2	6	12166	0.100	7.63×10^3	11.07	9.39	7.50	8.35
SMC-SMP3	4	9103	0.106	2.50×10^4	11.10	9.98	8.58	8.62
SMC-SMP4	5	12888	0.027	1.29×10^5	11.12	7.37	8.65	8.17
SMC-SMP5	5	9760	0.150	5.33×10^3	11.12	8.94	7.50	8.55
SMC-SMP6	4	12944	0.000	6.51×10^4	11.08	9.50	9.95	8.16
SMC-N87	8	11540	0.000	1.80×10^4	11.25	9.07	7.40	8.13

dances referred to the distances averaged over the ensemble of all PNe in a given ring: $\langle R^1 \rangle = 0.8$ kpc, $\langle R^3 \rangle = 4.9$ kpc, $\langle R^4 \rangle = 7$ kpc, and $\langle R^5 \rangle = 8.5$ kpc.

Figure 6 presents the dependences of the O abundance in bulge and thin-disk PNe on their mean Galactocentric distance obtained by the above method. The samples of thin-disk nebulae in Figs. 2a and 2b include only the type IIa and all type II nebulae, respectively. The oxygen abundance gradient $d[\text{O}/\text{H}]/dR$ in the former case (when only the type IIa nebulae are included in the sample) is -0.017 ± 0.01 dex kpc^{-1} , which is slightly higher than $d[\text{O}/\text{H}]/dR = -0.012$ dex kpc^{-1} obtained by Kholtygin and Milanova (2007) by analyzing the O abundance in all of the Galactic PNe belonging to the Galactic disk. When all type II nebulae are included in our sample, $d[\text{O}/\text{H}]/dR = -0.031 \pm 0.014$ dex kpc^{-1} . This value matches the

oxygen abundance gradient for PNe of the galaxy M31 (Garnett et al. 1997), which may be indicative of a similarity between our Galaxy and M31.

Analysis of Fig. 6 shows that the bulge objects continue the oxygen abundance–Galactocentric distance relation for the thin-disk nebulae. The following scenario can be suggested to explain the derived dependence. In accordance with the model by Immeli et al. (2004), the Galactic bulge is formed at early evolutionary phases of the Galaxy. After the bulge formation, the disk is formed starting from regions close to the bulge. Star formation then begins in regions farther from the Galactic center. Intense star formation both in the bulge and in the thin disk continues at least until an epoch no more than $(4-6) \times 10^9$ yr away from the present one. Unfortunately, since the errors in the gradient are significant, a larger sample of PNe than that considered here should be analyzed

to confirm the above conclusion. In this scenario, in accordance with the derived dependence in Fig. 6, the larger the Galactocentric distance of a star, the younger the age of the originally formed stars, while the O abundance decreases with increasing Galactocentric distance.

At present, a large number of extragalactic PNe are accessible to spectroscopic observations. High-quality spectra that can be modeled using the procedure described above have been obtained for the nearest (LMC and SMC) nebulae. The modeling results are partly presented in Table 6. More complete data on the elemental abundances in PNe of the Magellanic Clouds will be presented in the next publications. Figures 5b and 5c compare the He, C, N, and O abundances in PNe of the Galactic halo and the Magellanic Clouds. A similarity between the elemental abundances in these objects can be seen from Fig. 5, which may be indicative of their identical evolutionary age.

Our determinations of the parameters for Galactic and extragalactic PNe were used to update our electronic catalog of PNe parameters compiled previously (Kholtygin and Milanova 2008). The He, C, N, and O abundances that we derived here and other parameters for more than 120 nebulae of our Galaxy and the Magellanic Clouds were added to the updated catalog. For the nebulae whose spectra taken in the last 5–7 years were absent in the literature, we used the calculations of other authors presented in papers published no earlier than 1994. The Ne, S, Cl, and Ar abundance estimates presented in the new catalog were also taken from these papers.

When the abundance of the same element in a given PN was determined in several papers (the difference did not exceed 0.3 dex), we took its mean value as the sought-for abundance. If, however, the abundance differences exceeded this value, then we used only the data from papers published after 2001.

In addition to the abundances, the catalog presents the Galactic coordinates of PNe, their heliocentric and Galactocentric distances, their heights above the Galactic plane that we calculated by assuming the Galactocentric distance of the Sun to be 7.7 kpc (Nikiforov and Bobrova, 1999), the types of PNe, and the masses of their central stars. The sources of the observed line intensities in the PNe spectra and nebular parameters can be found in the cited catalog.

CONCLUSIONS

Here, using new observational data, we redetermined the He, C, N, and O abundances in more than 120 PNe of our Galaxy and the Magellanic Clouds.

The following conclusions can be drawn from our analysis of the results.

(1) The errors in the parameters of nebulae and their elemental abundances are determined mainly by the inaccuracies in measuring the observed line intensities. The He abundance is determined with an accuracy of 10–15%, while the errors in the derived C, N, and O abundances are 0.1–0.2 dex. Including the inaccuracies in the ionization corrections for the ionization stages of the chemical elements whose lines are absent in the nebular spectra increases the errors in the He abundance to 0.06 dex and in the C, N, and O abundances to 0.3 dex.

(2) Analysis of the distribution function for the parameter t^2 when it is determined from an analysis of the spectrum for the nebula NGC 7027 shows the possible presence of two components: the first and the second may correspond to the contribution from the large-scale and small-scale temperature variations in the nebula, respectively.

(3) Having analyzed the elemental abundances of various Galactic subsystems, we concluded that the Galactic bulge objects might be similar to type II nebulae in Peimbert's classification, while the nebulae of the Magellanic Clouds might be similar to Galactic halo objects. We suggested a scenario for successive formation of the Galactic bulge and thin disk.

ACKNOWLEDGMENTS

This study was supported by the Program of the Russian President for Support of Leading Scientific Schools (project no. NSh-1318.2008.2).

REFERENCES

1. L. H. Aller and S. J. Czyzak, *Astrophys. Space Sci.* **62**, 397 (1979).
2. L. H. Aller and S. J. Czyzak, *Astrophys. J. Suppl. Ser.* **51**, 211 (1983).
3. L. Aller and U. Liller, *Nebulae and Interstellar Matter*, Ed. by B. Middlehurst and L. Aller (Mir, Moscow, 1966; Univ. of Chicago, Chicago, 1968), p. 30.
4. Z. Brandt, *Statistical Methods of Observation Analysis* (Mir, Moscow, 1975), p. 312.
5. K. V. Bychkov and A. F. Kholtygin, *Elementary Processes in Astrophysical Plasma* (Gos. Aastron. Inst. MGU, Moscow, 2007), p. 186.
6. W. A. Feibelman, S. Hyung, and L. H. Aller, *Mon. Not. R. Astron. Soc.* **278**, 625 (1996).
7. D. R. Garnett, G. A. Shields, G. A. Skillman, et al., *Astrophys. J.* **489**, 63 (1997).
8. V. V. Golovatyj, A. Sapor, T. Feklistova, and A. F. Kholtygin, *Astron. Astroph. Trans.* **12**, 85 (1997).
9. R. Gruenwald and S. M. Viegas, *Astron. Astrophys.* **303**, 535 (1995).

10. G. A. Gurzadyan, *Planetary Nebulae* (Nauka, Moscow, 1962; Gordon & Breach, New York, 1970), p. 42 [in Russian].
11. S. Gutenkunst, J. Bernard-Salas, S. R. Pottash, et al., arXiv:0803.182v1 (2008).
12. J. P. Harrington, M. J. Seaton, S. Adams, et al., *Mon. Not. R. Astron. Soc.* **199**, 517 (1982).
13. R. B. C. Henry, *Origin and Evolution of the Elements, The Carnegie Observatories Centennial Symposia*, Ed. by A. McWilliam and M. Rauch (Cambridge Univ., Cambridge, 2004), p. 43.
14. F. Herwig, *Ann. Rev. Astron. Astrophys.* **43**, 435 (2005).
15. A. Immeli, M. Samland, O. Gerhard, et al., *Astron. Astrophys.* **413**, 547 (2004).
16. A. F. Kholtygin, *Astrofizika* **20**, 503 (1984).
17. A. F. Kholtygin, *Astron. Astrophys.* **329**, 691 (1998a).
18. A. F. Kholtygin, *Astrophys. Space Sci.* **255**, 513 (1998b).
19. A. F. Kholtygin, *Astrofizika* **43**, 627 (2000).
20. A. F. Kholtygin, J. C. Brown, J. P. Cassinelli, et al., *Astron. Astrophys. Trans.* **22**, 499 (2003).
21. A. F. Kholtygin and T. Kh. Feklistova, *Astron. Zh.* **69**, 960 (1992) [*Sov. Astron.* **36**, 496 (1992)].
22. A. F. Kholtygin and Yu. V. Milanova, http://www.astro.spbu.ru/staff/afk/GalChemEvol/-Neb_Ab.html; http://www.astro.spbu.ru/staff/afk/-GalChemEvol/ExtraGal_Ab.html (2008).
23. A. F. Kholtygin and Yu. V. Milanova, *Galaxy Evolution Across the Hubble Time*, IAU Symp. 235 (Cambridge Univ., Cambridge, 2007), p. 324.
24. X.-W. Liu, M. J. Barlow, M. Cohen, et al., *Mon. Not. R. Astron. Soc.* **323**, 343 (2001).
25. Yu. V. Luneva and A. F. Kholtygin, *Astrofizika* **45**, 451 (2002).
26. P. Marigo, *Astron. Astrophys.* **370**, 194 (2001).
27. F. Matteucci, arXiv:0804.1492v1 (2008).
28. J. Meléndez, M. Asplund, A. Alves-Brito, et al., *Astron. Astrophys.* **484**, L21 (2008).
29. Yu. V. Milanova and A. F. Kholtygin, *Pis'ma Astron. Zh.* **32**, 618 (2006) [*Astron. Lett.* **32**, 557 (2006)].
30. D. Minniti and M. Zoccali, *Formation and Evolution of Galaxy Bulges*, IAU Symp. 245 (in press); arXiv:0710.3104v1 (2007).
31. M. Niimura, S. J. Smith, and A. Chutjian, *Astrophys. J.* **565**, 645 (2002).
32. I. I. Nikiforov and A. Yu. Bobrova, *Kinem. Fiz. Nebesn. Tel Suppl.* **2**, 29 (1999).
33. C. Quireza, H. J. Rocha-Pinto, W. J. Maciel, *Astron. Astrophys.* **475**, 217 (2007).
34. M. Peimbert and R. Costero, *Boletín de los Observatorios de Tonantzintla y Tacubaya* **5**, 3 (1969).
35. M. Peimbert, *Planetary Nebulae*, IAU Symp. 76 (Reidel, Dordrecht, 1978), p. 215.
36. C. Rola and D. Pelat, *Astron. Astrophys.* **287**, 677 (1994).
37. C. Rola and G. Stasinska, *Astron. Astrophys.* **282**, 199 (1994).
38. R. H. Rubin, *Astrophys. J.* **155**, 841 (1969).
39. R. H. Rubin, *Astrophys. J. Suppl. Ser.* **69**, 897 (1989).
40. L. Stanghellini, M. A. Guerrero, K. Cunha, et al., *Astrophys. J.* **651**, 898 (2006).
41. Y. G. Tsamis, M. J. Barlow, X.-W. Liu, et al., *Mon. Not. R. Astron. Soc.* **345**, 186 (2003).
42. Y. G. Tsamis, J. R. Walsh, D. Pequignot, et al., *Mon. Not. R. Astron. Soc.* **86**, 22 (2008).
43. W. Wang and X.-W. Liu, *Mon. Not. R. Astron. Soc.* **389**, L33 (2008).
44. Y. Zhang, X.-W. Liu, S.-G. Luo, et al., *Astron. Astrophys.* **442**, 249 (2005).
45. M. Zoccali, A. Lecœur, B. Barbuy, et al., *Astron. Astrophys.* **457**, L1 (2006).

Translated by V. Astakhov